

**“Azdiracthta Indica leaves extract as green inhibitor for  
aluminium corrosion protection in NaOH solution”**

**B. M. Patel**

**Research Scholar**

**Department of Chemistry,**

**C. B. Patel Computer College & J. N. M. Patel Science College,  
Surat 395017, Gujarat, India.**

**V. R. Patel**

**Research Scholar**

**Department of Chemistry,**

**C. B. Patel Computer College & J. N. M. Patel Science College,  
Surat 395017, Gujarat, India.**

**D. M. Patel**

**Research Scholar**

**Department of Chemistry,**

**C. B. Patel Computer College & J. N. M. Patel Science College,  
Surat 395017, Gujarat, India.**

**N. I. Prajapati**

**Research Scholar**

**Department of Chemistry,**

**C. B. Patel Computer College & J. N. M. Patel Science College,  
Surat 395017, Gujarat, India.**

**K. K. Patel**

**Assistant Professor**

**Department of Chemistry, Shri Govind Guru University,  
Godhra 388713, Gujarat, India.**

**S. A. Desai**

**Research Guide**

**Department of Chemistry,**

**C. B. Patel Computer College & J. N. M. Patel Science College,  
Surat 395017, Gujarat, India.**

**\*Corresponding Author Email: [desai.sagar@hotmail.com](mailto:desai.sagar@hotmail.com)**

**Mo: 9825127809**

## **Abstract:**

The corrosion inhibition of aluminium in NaOH solution by *Azadirachta indica* leaves extract (AILE) as a green inhibitor has been studied using weight loss, temperature effect, kinetic study, Potentiodynamic Polarization (PDP), Electrochemical Impedance Spectroscopy (EIS), Scanning Electron Microscope (SEM), and Energy Dispersive X-ray Spectroscopy (EDX) techniques. As inhibitor concentration increases, corrosion rate decreases while efficiency of inhibition (I.E.) increases. Corrosion rate increases with the increase in temperature. Mechanism of inhibition was also investigated by calculating the thermodynamic parameters like ( $\Delta G$ ), ( $Q_{ads}$ ), ( $E_a$ ), ( $\Delta H_{ads}$ ) and ( $\Delta S_{ads}$ ). Physisorption of extract is agree well with the Langmuir adsorption model. Maximum I.E. of *Azadirachta indica* extract was found up to 90.74 % at 2.0 gm/dL inhibitor concentration in 0.05 N NaOH solution. The virtually semicircular Nyquist plot graph indicates that aluminium corrosion is mostly inhibited by the charge transfer process. The thermodynamic and kinetic characteristics for the tested system were computed using the data collected at different temperatures (313K, 323K, and 333K). The Langmuir adsorption isotherm was followed by the inhibitor molecules' adsorption on the aluminium surface. The findings demonstrated that an extract from *Azadirachta indica* leaves successfully prevents aluminium corrosion in a NaOH solution. The present study indicates that *Azadirachta indica* leaves extract is a good eco-friendly inhibitor for the corrosion of aluminium in NaOH base medium.

## **1. Introduction:**

One of the most significant national issues is corrosion, especially in light of civilisation's, fast industrialisation and advancement. Due to its numerous great qualities, including its low density, high ductility, superior electrical and thermal conductivities, cost and availability for the fabrication and construction industries, and good corrosion resistance, aluminium is a valuable metal in many industries.

Aluminium is a low cost metal and shows its desirable properties, like high energy density, a high negative potential. The electrochemical behaviour of aluminium in alkaline solutions has been studied in order to develop aluminium as an anode in metal/air batteries. It has been demonstrated that when aluminium is used as a galvanic anode in sodium hydroxide solution, corrosion inhibitors greatly reduce the quantity of metal wasted as a result of self-corrosion [1-5]. Recent research has examined the potential of naturally occurring chemicals produced from plants to regulate corrosion, with promising results showing high inhibitory efficacy. This topic of study is important because natural products are inexpensive, readily available, ecologically friendly, and renewable sources of materials.

Plant materials have been utilised as corrosion inhibitors, including leaves, bark, seeds, flowers, and roots. Plant-based products are inexpensive, readily available, non-toxic, biodegradable, and environmentally benign [6-9].

*Azadirachta indica* (AZI) is a common multipurpose tree that can be used in Ayurvedic and traditional medicine, as well as in organic farming and cosmetics [10]. Neem, or *Azadirachta indica*, is a member of the Meliaceae family. Tannins, phenolic compounds, alkaloids, carbohydrates, reducing flavonoids, glycosides, and saponins were all found in the phytochemical examination of *Azadirachta indica* leaf extract [11].

Below mentioned reported work of AILE shows good inhibition efficiency for different metal for various corrosive environment;

Metal	Corrosive Environment	Reference
Aluminium (AA 1060)	HCl	Abakedi and Asuquo [12]
Aluminium Alloy (AI-3102)	MB & MC Bacteria media	Selvam et al. [13]
Zinc	HCl, NaOH	Ameh et al. [14]
Carbon steel	HCl, NH <sub>4</sub> Cl	Loto and Akpanyung [15]
Carbon steel	H <sub>2</sub> SO <sub>4</sub>	Malarvizhi et al. [6]
Brass	HNO <sub>3</sub>	Patel and Vashi [17]
Copper	HNO <sub>3</sub>	Patel and Vashi [18]
Mild Steel	HCl	Ade et al. [19]

The present work aims to investigate the inhibition efficiency of AILE for the corrosion of aluminium in alkaline medium by chemical and electrochemical techniques. It is also aimed to study the effect of temperature on the corrosion rate of aluminium.

## 2. MATERIAL AND METHODS

### 2.1 Preparation of sample:

The aluminium specimens with a chemical composition of 99.15 % Al, 0.53 % Fe, 0.17 % Cu, 0.15 % Zn, with a small of 6 mm diameter near the upper edge were used in the present study. The metal specimens of size 5.47cm x 2.57cm x 0.2 cm, having an effective area of 0.3041 dm<sup>2</sup> were used.

### 2.2 Corrosive Medium:

The most common use for inhibitors is in aluminium-alkaline solution systems, which are used in industrial operations including pickling, etching, and alkaline cleaning, as well as to increase the efficiency of aluminium devices. The corrosion medium having concentrations of 0.05, 0.10 and 0.15 N was prepared by diluting analytical grade of NaOH purchased from Merck using double-distilled water[20].

### 2.3 Preparation of Azadirachta indica leaves extract (AILE):

Fresh leaves of Azadirachta indica leaves were collected from local site near by Binwada, Valsad, Gujarat. Leaves were plucked, carefully washed and shade-dried and then dried in hot air oven at 50°C before ground into fine powder. AILE was prepared by refluxing 10.0 gm of Azadirachta indica leaves powder with 100 mL of double-distilled water for about 2 hours then filtered, and this solution is used to prepare the required inhibitor concentrations (0.8, 1.2, 1.6 and 2.0 gm/dL).



Fig : 1 Azadirachta indica leaves

### 2.4 Weight loss measurements:

Aluminium specimens having an area of 0.3041 dm<sup>2</sup> were each suspended in 230 ml of 0.05, 0.10 and 0.15 N NaOH solution in absence and presence of 0.8, 1.2, 1.6 and 2.0 gm/dL concentration of AILE using glass hooks at 301 ± 1 K for an immersion period of 24h. After 24h specimens were retrieved from beaker, washed with distilled water, dried well and reweighed. From the weight loss data, corrosion rate (CR) was calculated using following equation:

$$\text{C. R. } \left( \frac{\text{mg}}{\text{dm}^2\text{d}} \right) = \frac{\text{Weight loss (gm)} \times 1000}{\text{Effective Surface area(dm}^2\text{)} \times \text{time (day)}} \quad \dots(1)$$

Inhibition efficiency (I. E.) was calculated by using the following equation:

$$\text{I. E. (\%)} = \left\{ \frac{(W_u - W_i)}{W_u} \right\} \times 100 \quad \dots(2)$$

Where,  $W_u$  = Weight loss in the absence of inhibitor,  $W_i$  = Weight loss in the presence of inhibitor.

The degree of surface coverage ‘ $\theta$ ’ of the aluminium specimen for different concentration of NaOH solution have been evaluated by weight loss experiments using the following equation.

$$\theta = \frac{(W_u - W_i)}{W_i} \quad \dots(3)$$

### 2.5 Temperature effect:

To study the effect of temperature on corrosion rate, aluminium specimens were completely immersed in 230 ml of 0.15 N NaOH solution without and with different concentrations of AILE at 313, 323 and 333 K for 2h.

## **2.6 Scanning Electron Microscope (SEM) measurements:**

The aluminium plates surface was examined using a high-energy electron beam scan. When the metal plate is exposed to a high-energy electron beam, it emits a variety of signals, such as secondary electrons, back-scattered electrons, absorbed electrons, transmitted electrons, cathode luminescence, and X-rays. This method primarily uses secondary electron signals to capture an image of the metal plate, both with and without the inhibitor. For 24 hours, the aluminium plates were fully submerged in 230 mL of 0.15 N NaOH solution at room temperature ( $301 \pm 1$  K).

## **2.7 Energy dispersive x-ray spectroscopic (EDX) measurements:**

The elements on the aluminium surface are determined using EDX spectra following a 24-hour immersion time in 0.15 N NaOH with and without a 2.0 gm/dL solution of green inhibitor.

## **2.8 Potentiodynamic Polarization (PDP) measurement:**

A potentiostat/galvanostat meter [Instruments: GAMRY-Reference 600] was used for PDP and EIS investigations. The reference electrode in this experiment was Ag/AgCl, the auxiliary electrode was platinum, and the working electrode was aluminium metal. Aluminium specimens having an area of  $1 \text{ cm}^2$  immersed in 230 mL of 0.05 N NaOH with and without different inhibitors in order to conduct the polarization measurement. The corrosion current density ( $I_{\text{corr}}$ ) is calculated by drawing Tafel lines to the corresponding corrosion potentials ( $E_{\text{corr}}$ ) [21]. Anodic Tafel slope ( $\beta_a$ ) and cathodic Tafel slope ( $\beta_c$ ) were computed.

## **2.9 Electrochemical impedance spectroscopic (EIS) measurements:**

For EIS analysis, potentiodynamic polarization experiment methodology were used. A constant AC voltage with a wide frequency range of 1 to 100 kHz and a small amplitude of 5.0 mV was supplied to the system. A graph of real impedance ( $Z'$ ) vs imaginary impedance ( $Z''$ ) was fashioned. The Nyquist plots were used to compute the charge transfer resistance ( $R_{\text{ct}}$ ) and double-layer capacitance ( $C_{\text{dl}}$ ). Impedance measurements were carried out both with and without inhibitors.

# **3. RESULTS AND DISCUSSION**

## **3.1 Weight loss experiments**

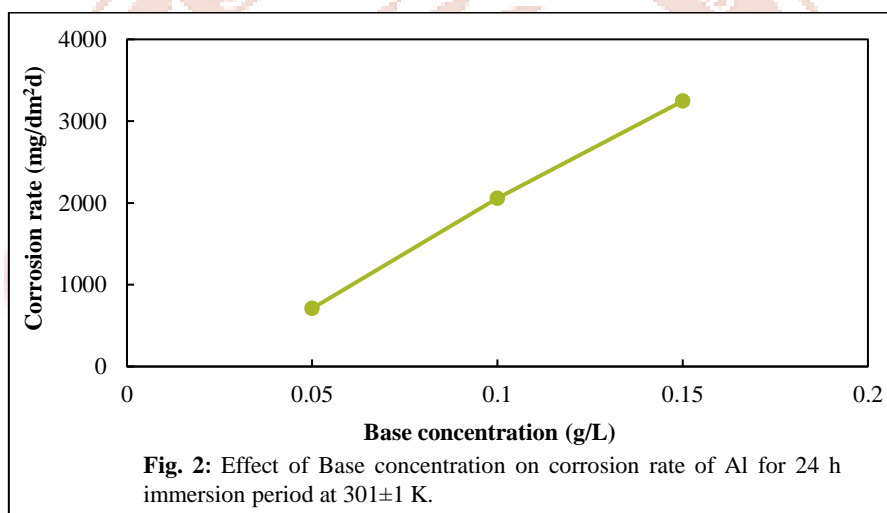
### **3.1.1 Effect of base concentration:**

Results showed in Fig. 2 indicates that as the base concentration increases corrosion rate increases. Corrosion rate was 710.29, 2058.53 and 3245.64 mg/dm<sup>2</sup>.d corresponding to

0.05, 0.10 and 0.15 N NaOH concentration respectively for an exposure period of 24 h at  $301 \pm 1$  K (Table 1).

**Table 1:** Inhibition efficiency (I.E.), Corrosion rate of AILE on Al in 0.05, 0.10 and 0.15 N NaOH for an immersion period of 24h at  $301 \pm 1$  K.

Inhibitor	Inhibitor Concentration (C) gm/dL	0.05 N NaOH		0.10 N NaOH		0.15 N NaOH	
		C. R. mg/dm <sup>2</sup> .d	I. E. (%)	C. R. mg/dm <sup>2</sup> .d	I. E. (%)	C. R. mg/dm <sup>2</sup> .d	I. E. (%)
Blank	-	710.29	-	2058.53	-	3245.64	-
AILE	0.8	180.86	74.54	591.91	71.25	1585.00	51.17
	1.2	154.55	78.24	480.11	76.68	1321.93	59.27
	1.6	105.23	85.19	365.01	82.27	963.50	70.31
	2.0	65.77	90.74	276.22	86.58	720.16	77.81



### 3.1.2 Effect of inhibitor concentration:

From the results, corrosion rate was 710.29 mg/dm<sup>2</sup>, 2058.53 mg/dm<sup>2</sup> and 3245.64 mg/dm<sup>2</sup> for 0.05N, 0.10N and 0.15N NaOH concentrations respectively for an immersion period of 24 h at 303 K, indicates that as the base concentration increases, the corrosion rate increases. The highest I. E. (%) was found 90.74 % in 0.05N NaOH solution at 2.0 g/dl AILE inhibitor concentration (Table 1). As the concentration of inhibitors increases I.E. increases at constant base concentration (Table 1, Fig. 3). Rate constant decreases whereas half-life increases at constant base concentration (Table 2). A straight line indicating that the inhibitor followed the Langmuir adsorption isotherm (Fig. 4).

**Table 2:** Kinetic data for the corrosion of aluminium in various concentration of NaOH containing *AILE* as a green inhibitor. (Calculated from the weight loss data)

**Effective area of specimen: 0.3041 dm<sup>2</sup>**

**Immersion Period: 24 h**

**Temperature: 303 ± 1 K**

Inhibitor	Inhibitor Conc. (C) gm/dL	0.05 N NaOH				0.10 N NaOH				0.15 N NaOH			
		Rate Constant (K) (K x 10 <sup>-3</sup> )	Half-life (t <sub>1/2</sub> )	Surface Coverage (θ)	(C/θ)	Rate Constant (K) (K x 10 <sup>-3</sup> )	Half-life (t <sub>1/2</sub> )	Surface Coverage (θ)	(C/θ)	Rate Constant (K) (K x 10 <sup>-3</sup> )	Half-life (t <sub>1/2</sub> )	Surface Coverage (θ)	(C/θ)
Blank	-	30.36	22.82	-	-	90.70	7.64	-	-	146.96	4.72	-	-
<i>AILE</i>	0.8	7.65	90.60	0.745	1.073	25.25	27.44	0.712	1.123	69.09	10.03	0.512	1.564
	1.2	6.53	106.08	0.782	1.534	20.44	33.91	0.767	1.565	57.31	12.09	0.593	2.025
	1.6	4.44	155.92	0.852	1.878	15.50	44.72	0.823	1.945	41.45	16.72	0.703	2.276
	2.0	2.78	249.71	0.907	2.204	11.71	59.17	0.866	2.310	30.79	22.51	0.778	2.570

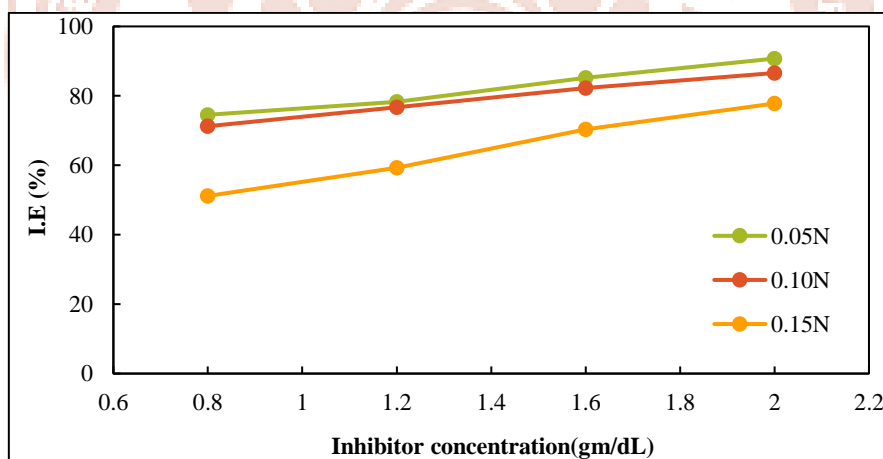


**Fig. 3:** Inhibition efficiency (I.E.) of Al corrosion in 0.05, 0.10 and 0.15 N NaOH solution in presence of different concentration *AILE* for an immersion period of 24 h.

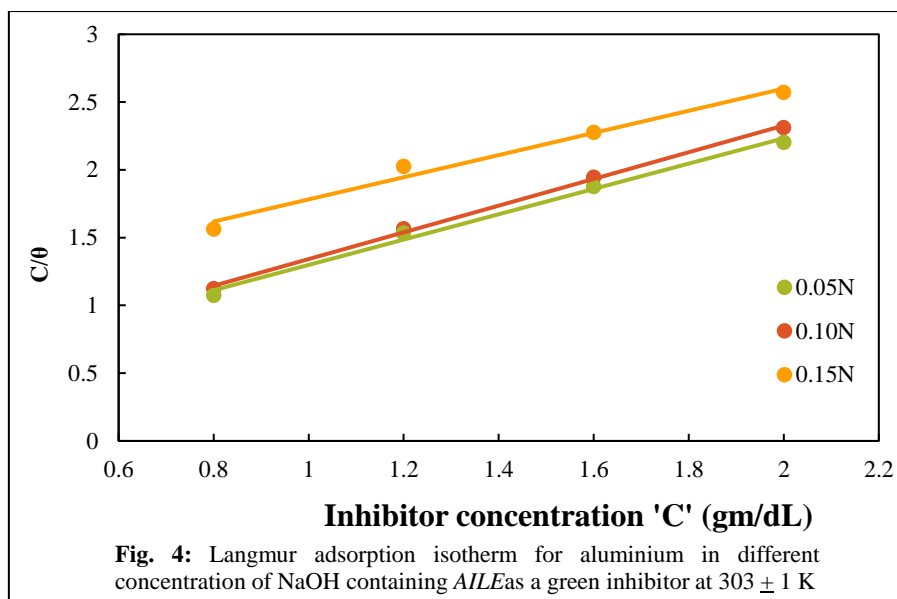


**Fig. 4:** Langmuir adsorption isotherm for aluminium in different concentration of NaOH containing *AILE* as a green inhibitor at  $303 \pm 1$  K

### 3.1.3 Temperature effect:

To investigate the influence of temperature on corrosion of aluminium, the weight loss experiments were also carried out at 313, 323 and 333 K temperatures in 0.15 N NaOH in absence and presence of AILE for an immersion period of 2h (Table 3). The corrosion rate increases with rise in temperature. Corrosion rate was 13061.49, 20046.04 and 28885.24 mg/dm<sup>2</sup>.d corresponding to 313,323 and 333 K respectively. Corrosion rate increases with temperature may be due to the desorption of the adsorbed molecules inhibitor and/or aggressive at higher temperature and thus exposing the fresh metal surface to further attack [22], which results in intensification of the kinetic of electrochemical reaction [23] and thus explains the higher corrosion rate at elevated temperature. The addition of AILE in corrosive media indicates that as the temperature increases, I.E. decreases (Table 3, Fig. 5) at constant inhibitor concentration. So, raise in the temperature, the inhibitor's effectiveness significantly reduce.

**Table 3:** Temperature effect on corrosion rate (CR) and inhibition efficiency (I.E. %) for aluminium in 0.15 N NaOH in the absence and presence of *AILE* for an immersion period of 2 h.

Effective area of specimen: 0.3041 dm <sup>2</sup>		Immersion Period: 2 h					
Inhibitor	Inhibitor concentration 'C'	Temperature					
		313 K		323 K		333 K	
	gm/dL	CR mg/dm <sup>2</sup> .d	I.E. (%)	CR mg/dm <sup>2</sup> .d	I.E. (%)	CR mg/dm <sup>2</sup> .d	I.E. (%)
Blank	-	13061.49	-	20046.04	-	28885.24	-
<i>AILE</i>	0.8	4695.82	64.05	9233.80	53.94	15073.99	47.81
	1.2	4143.37	68.28	7773.76	61.22	12982.57	55.05

	1.6	3235.78	75.23	6866.16	65.75	11325.22	60.79
	2.0	2367.64	81.87	4537.98	77.36	10378.17	64.07

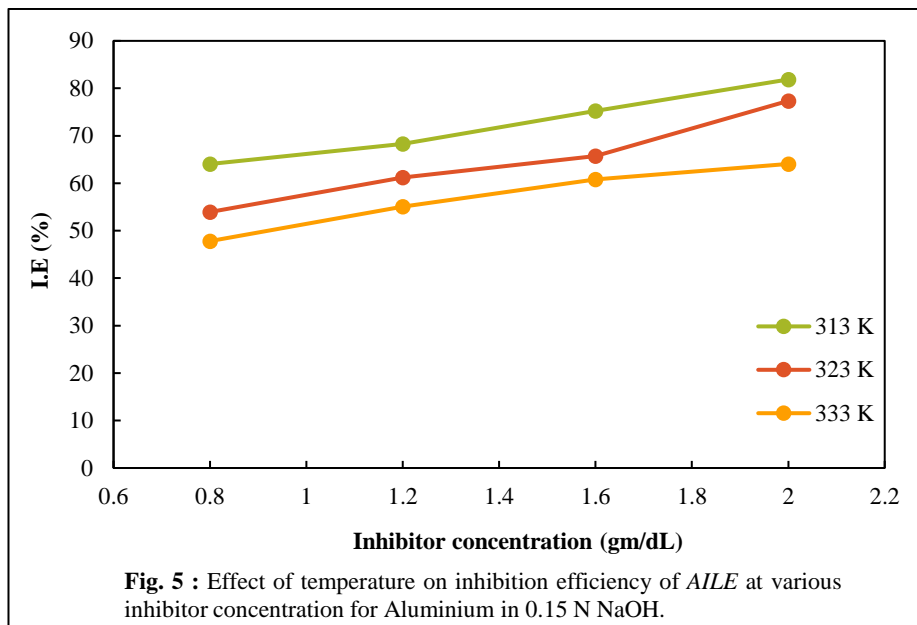


**Fig. 5 :** Effect of temperature on inhibition efficiency of *AILE* at various inhibitor concentration for Aluminium in 0.15 N NaOH.

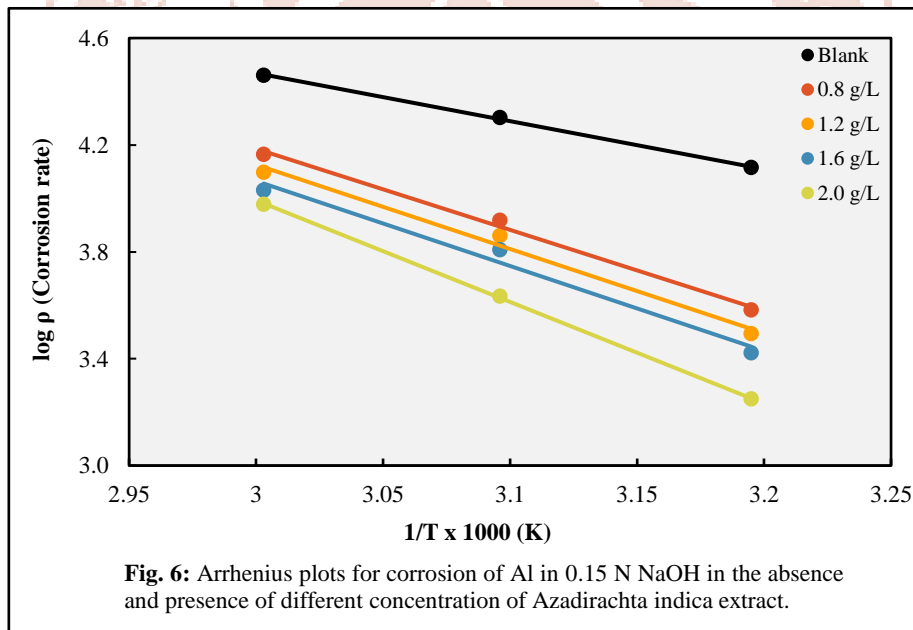


**Fig. 6:** Arrhenius plots for corrosion of Al in 0.15 N NaOH in the absence and presence of different concentration of *Azadirachta indica* extract.

### 3.1.4 Thermodynamic and Kinetic parameters:

#### (a) Energy of activation ( $E_a$ ):

The value of energy of activation ( $E_a$ ) has been calculated with the help of Arrhenius equation [24].

$$\log \frac{\rho_2}{\rho_1} = \frac{E_a}{2.303 R} \left( \frac{1}{T_1} - \frac{1}{T_2} \right) \quad \dots(4)$$

Where,  $\rho_1$  and  $\rho_2$  represent the corrosion rate at temperatures  $T_1$  and  $T_2$ , respectively. The results presented in Table 4 show that the values of  $E_a$  were higher in the inhibited base (ranging from 49.35 to 64.31 kJ/mol) than in the uninhibited base (34.32 kJ/mol), indicating physical

adsorption of the inhibitor on the metal surface, which raises the process's  $E_a$  value [25]. The slope of the Arrhenius plot of  $\log \rho$  vs  $1/T \times 1000$  (Fig. 6), which is in good agreement with the computed values for inhibited system.

**(b) Heat of adsorption ( $Q_{ads}$ ):**

The values of heat of adsorption ( $Q_{ads}$ ) were calculated by using the following equation [26].

$$Q_{ads} = 2.303 R \left[ \log \left( \frac{\theta_2}{1-\theta_2} \right) - \log \left( \frac{\theta_1}{1-\theta_1} \right) \right] \left[ \frac{T_1 T_2}{T_2 - T_1} \right] \quad \dots(5)$$

The fraction of the metal surface covered by the inhibitor at temperatures  $T_1$  and  $T_2$  is denoted by  $\theta_1$  and  $\theta_2$ , respectively. It is clear that the values of  $Q_{ads}$  were negative in every instance, ranging from -19.10 to -58.17 kJ/mol. The negative values of  $Q_{ads}$  indicate that when the temperature rises, the adsorption process and, consequently, the I.E. decrease, validating the physisorption mechanism [27-28].

**(c) Adsorption isotherms:**

The interaction between the metal and inhibitor as well as the adsorption equilibrium were examined using an adsorption isotherm analysis. The adsorption isotherm can be used to give basic details about how inhibitors interact with a metal surface [29].

Inhibitor molecules slow down corrosion by blocking the reaction sites through adsorption. Equation 3 was used to determine the surface coverage " $\theta$ " value. The system follows the Langmuir adsorption isotherm, as shown by Fig. 4 plot of inhibitor concentration ' $C$ ' vs ' $C/\theta$ ', which produces a straight line with slope values equal to unity [30]. This isotherm can be represented as;

$$\frac{C}{\theta} = \frac{1}{K_{ads}} + C \quad \dots(6)$$

Where,  $K_{ads}$  is the equilibrium constant and  $C_{inh}$  is the inhibitor concentration.

**(d) Free energy of adsorption ( $\Delta G^{\circ}_{ads}$ ):**

The Langmuir isotherm, represented by a plot of  $C/\theta$  vs  $C$ , was used to calculate  $\Delta G^{\circ}_{ads}$  (Fig.4).  $K_{ads}$  can be computed from the intercepts of the straight line on the  $C/\theta$  axis, which was connected to  $\Delta G^{\circ}_{ads}$  according to the following formula [31-32].

$$\Delta G^{\circ}_{ads} = -RT \ln (55.5 K_{ads}) \quad \dots(7)$$

Where,  $R$  = Gas constant,  $T$  = Temperature,  $K_{ads}$  = Equilibrium constant, and 55.5 represent the molar constant of water in the solution. The mean  $\Delta G^{\circ}_{ads}$  value was negative (-11.88 kJ/mol), suggesting that strong interaction of inhibitor and spontaneous adsorption of inhibitor molecule on the metal surface. Similar observation was recorded by Desai and Patel [33, 34]. The values of  $\Delta G^{\circ}_{ads}$  -20 kJ/mol are compatible with physisorption, whereas values of -40 kJ/mol or above are linked to chemisorptions [35].

**(e) Enthalpy of adsorption ( $\Delta H^{\circ}_a$ ):**

The values of  $\Delta H^{\circ}_a$  were positive and increased when the inhibitor was present (Table 4), indicating a better level of surface coverage and higher protection efficiency reached because the energy barrier for the corrosion reaction to occur was raised [36]. The endothermic nature of the reaction is indicated by the positive enthalpy change  $\Delta H^{\circ}_a$ , which ranged from 41.09 to 71.24 kJ/mol, suggesting that a higher temperature favours the corrosion process [37].  $\Delta H^{\circ}_a$  was calculated using the following equation;

$$\Delta H^{\circ}_a = E_a - RT \quad \dots(8)$$

**(f) Entropy of adsorption ( $\Delta S^{\circ}_a$ ):**

$\Delta S^{\circ}_a$  were calculated using below equations [38].

$$\Delta S^{\circ}_a = [\Delta H^{\circ}_a - \Delta G^{\circ}_a] / T \quad \dots(9)$$

A positive value of  $\Delta S^{\circ}_a$  between 0.035 and 0.256 kJ/mol implies an entropically favourable corrosion process [39].

**(g) Rate constant (k) and Half- life (t1/2):**

The half-life increases while the rate constant k decreases as the inhibitor concentration rises. This outcome was consistent with the findings of Talati and Modi [40]. As Base concentration rises, so does the corrosion rate constant 'K' (Table 2). The following formula was used to determine the half-life (t1/2) values [41].

$$t_{1/2} = 0.693 / k \quad \dots(10)$$

Where, 't' is time in hours and 'k' is rate constant.

**Table-4:** Thermodynamic parameters of Al in 0.15 N NaOH in absence and presence of *AILE* as green inhibitor.

Inhibitor concentration (gm/dL)	Energy of activation ( $E_a$ ) (kJ/mol)		Heat of adsorption ( $Q_{ads}$ ) (kJ/mol)		Free energy of adsorption ( $\Delta G^{\circ}_{ads}$ ) (kJ/mol)				Enthalpy of adsorption ( $\Delta H^{\circ}_a$ ) (kJ/mol)		Entropy of adsorption ( $\Delta S^{\circ}_a$ ) (kJ/mol)	
	Mean From Eq. (4)	From Arrhenius Plot	313-323 K	323-333 K	313 K	323 K	333 K	Mean	313 K	323 K	313 K	323 K
Blank	34.32	34.41	-	-	-	-	-	-	33.34	29.93	-	-
0.8	50.31	50.61	-35.28	-21.94	-12.20	-11.41	-12.02	-11.88	54.16	41.09	0.212	0.035
1.2	49.35	49.53	-26.06	-22.69					50.21	43.13	0.199	0.169

1.6	53.97	54.38	-38.56	-19.10					60.55	42.0 2	0.23 2	0.165
2.0	64.31	63.94	-23.45	-58.17					52.01	71.2 4	0.20 5	0.256

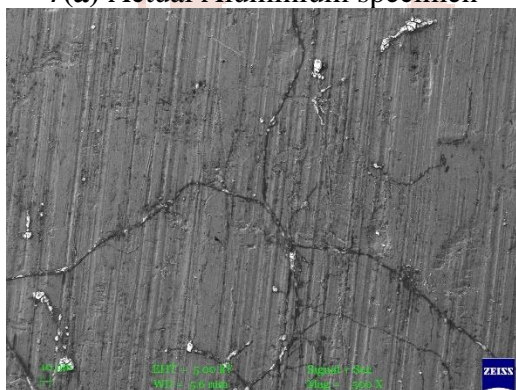
### 3.1.5 Scanning Electron Microscope (SEM) measurements:

Scanning Electron Microscopy (SEM) was used to examine the surface morphology of aluminium specimens after they were submerged in a 0.15 N NaOH solution, both with and without extract from AILE. The aluminium surface in the blank NaOH solution showed signs of significant damage, including pits, cracks, and porous morphology. This suggests that hydroxide ions were strongly attacking the protective oxide covering. The following is a representation of the corrosion response of aluminium in an alkaline medium:

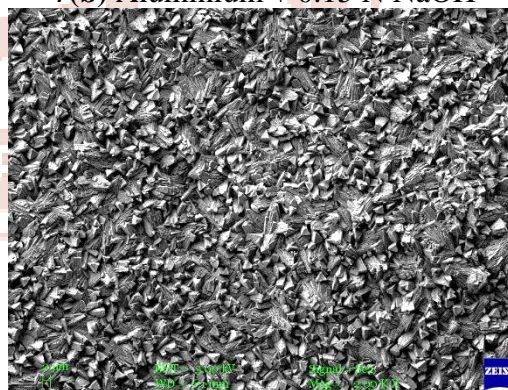


This reaction demonstrates how easily aluminium dissolves in NaOH to produce soluble sodium aluminate ( $\text{Na}[\text{Al}(\text{OH})_4]$ ), which is accompanied by the evolution of hydrogen gas. As a result of ongoing metal disintegration and film breakup, the surface becomes uneven and rough. On the other hand, when AILE is present, the aluminium surface has a relatively smoother morphology with fewer pits and fissures. This shows that the organic substances found in the AILE, such as flavonoids, tannins, saponins, and alkaloids, have formed a protective adsorbed layer. Polar functional groups with O and N atoms allow these phytochemical components to be adsorbed on the aluminium surface, creating a thin, compact layer that reduces metal dissolution and limits hydroxide ion attack.

7(a) Actual Aluminium specimen



7(b) Aluminium + 0.15 N NaOH



7(c) Aluminium + 0.15 N NaOH + AILE

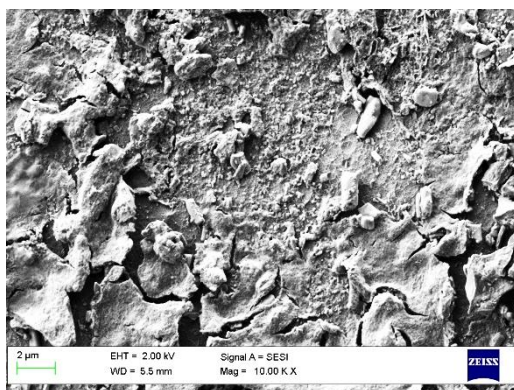


**Fig. 7:** SEM micrographs of Aluminium specimen;  
**7(a)** Actual unexposed Aluminium specimen,  
**7(b)** Aluminium specimen immersed in 0.15 N NaOH,  
**7(c)** Aluminium specimen immersed in 0.15 N NaOH with 2.0 gm/dL *AILE*

### 3.1.6 Energy dispersive X-ray spectroscopic (EDX) measurements:

The primary constituents of green inhibitors are carbon and oxygen, which are mostly present in the structures of flavonoids, alkaloids, terpenoids, tannins, saponins, and steroids, as indicated by the atomic weight% of the chemical elements recorded in EDX in Table 5. EDX spectrum of aluminium in 0.15 N NaOH reveals oxygen peaks with a significant amount of aluminium and a high percentage of oxygen, suggesting that aluminium oxide production is the mechanism by which aluminium corrodes (Fig. 8b). When compared to the blank spectrum, the EDX spectra of the inhibited sample (Fig. 8c) revealed a low percentage of oxygen, indicating that the inhibitor molecule tightly binds to the aluminium surface to prevent corrosion and the development of aluminium oxide.

**Table 5:** Percentage of different elements composing the Aluminium surface obtained by EDX spectrum analysis.

System	Percentage of the atomic weight of elements		
	Al	O	C
Al	71.20	7.20	21.60
Al + NaOH	27.03	72.07	-
Al + NaOH + <i>AILE</i> (inhibitor)	58.03	5.00	36.07



**Fig. 8a: EDX images of the plain Aluminium surface**

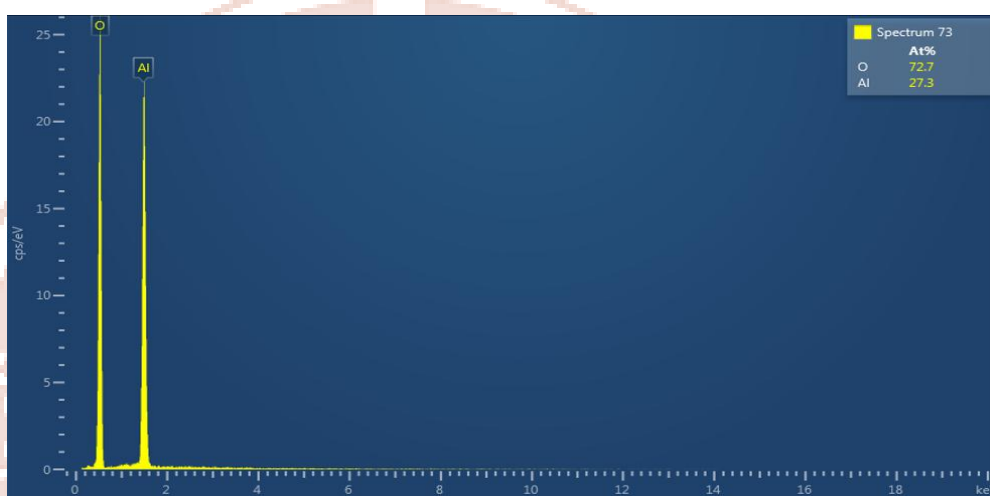


**Fig. 8b: EDX images of the Aluminium surface after 24 h of immersion at  $301 \pm K$  in 0.15N NaOH in the absence of inhibitor**



**Fig. 8c: EDX images of the Aluminium surface after 24 h of immersion at  $301 \pm K$  in 0.15 N NaOH in 2.0 gm/dL AILE.**

### 3.1.7 Potentiodynamic polarization measurements:

Potentiodynamic polarization is carried out in 0.05N NaOH, with and without green inhibitors. The different electrochemical parameters that are determined from the Tafel plot, including corrosion potential ( $E_{corr}$ ), corrosion current density ( $i_{corr}$ ), and the values of the Tafel parameters ( $\beta_a$ ,  $\beta_c$ , and  $\beta$ ) both anodic and cathodic polarization, whereas inhibitor curves exhibit more cathodic and minimal anodic polarization (Table 6, Fig. 9). The inhibitors cause a change in both the cathodic and anodic Tafel slopes.

The polarization study's inhibition efficiency (I.E.) was calculated by using the following formula;

$$I.E. (\%) = \frac{i_{corr(uninh)} - i_{corr(inh)}}{i_{corr(uninh)}} \times 100 \quad \dots(12)$$

Whereas  $i_{corr(inh)}$  denotes corrosion current density in inhibited base,  $i_{corr(uninh)}$  shows corrosion current density in uninhibited base.

Both the anodes and the cathodes are polarized according to the polarization curves. Typically, the inhibitor is either cathodic or anodic if the difference between  $E_{corr}$  and the blank is greater than 85 mV [45, 46]. The highest fluctuation of  $E_{corr}$  for the inhibitors in this study was -0.140 mV (Table 6), indicating that the inhibitors function as mixed-type inhibitors.

**Table 6:** Potentiodynamic polarization data and I.E. of AILE for Aluminium corrosion in 0.05 N NaOH at 301 K.

System	$E_{corr}$ (mV)	$I_{corr}$ ( $\mu\text{A}/\text{cm}^2$ )	Tafel slope (mV/decade)		Tafel Constan t $\beta$ (mV)	Inhibition Efficiency (%)	
			$+\beta_a$	$-\beta_c$		polarizati on method	Weight Loss method
Blank	-1.560	648.0	777.1	381.0	111.15	-	-
AILE	-1.420	8.130	263.2	190.8	48.09	98.74	90.74

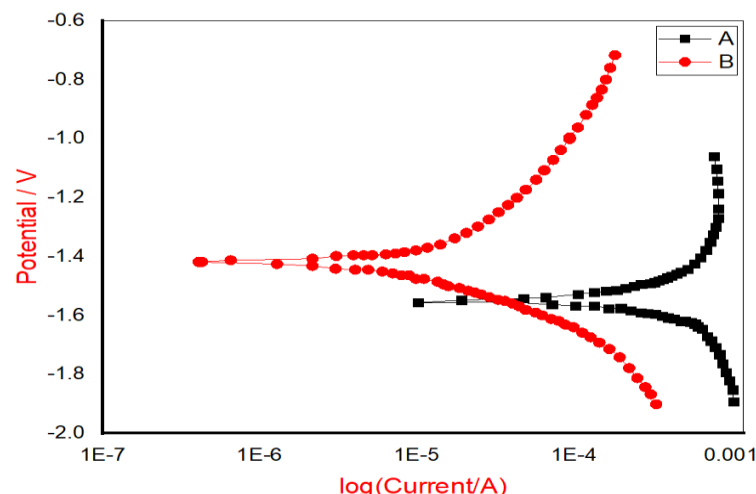


**Fig. 9:** Tafel polarization curves for Aluminium in 0.05 N NaOH without inhibitor (A) and with 2.0 g/dL AILE (B).

### 3.1.8 Electrochemical impedance spectroscopic (EIS) measurements:

EIS is a useful method for examining the interactions between metal surfaces and calculating the potential rate of corrosion. Nyquist plots (Fig. 10) for aluminium corrosion in a 0.05 N NaOH solution with and without an inhibitor were examined and results are shown in Table 7. When the inhibitor is present, the capacitive circle diameter is greater than when it is not. The high-frequency capacitive loop is associated with R<sub>ct</sub>. Inhibition efficiency (I.E.) from the EIS approach was computed using the following equation to determine the frequency at which the imaginary component of the impedance is highest in order to calculate C<sub>dl</sub> [47].

$$I. E. (\%) = \frac{C_{dl}(\text{uninh}) - C_{dl}(\text{inh})}{C_{dl}(\text{uninh})} \times 100 \quad \dots(13)$$

**Table 7:** EIS parameters for Aluminium corrosion in 0.05 N NaOH without and with 2.0g/dL AILE.

System	R <sub>ct</sub> ohm/cm <sup>2</sup>	C <sub>dl</sub> (μF/cm <sup>2</sup> )	Inhibition Efficiency (%)	
			By EIS method	By Weight Loss method
Blank	228.78	73.08	-	-
<i>Azadirachta indica</i>	4684.67	0.10018	99.86 %	90.74 %

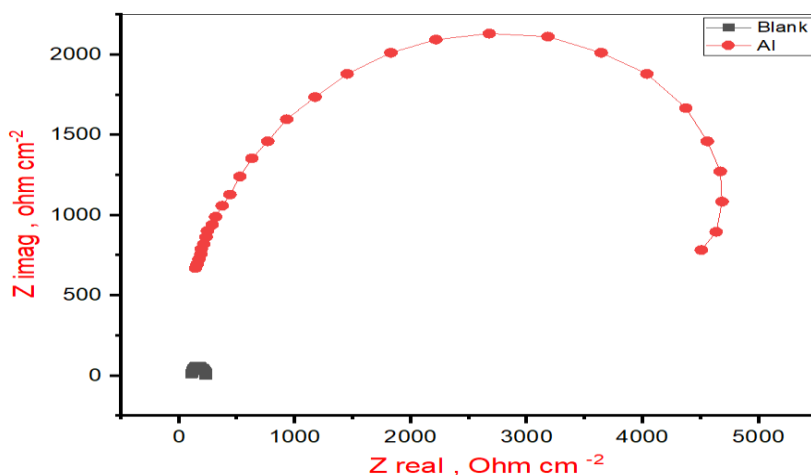


**Fig. 10:** ESI curves for Aluminium in 0.05 N NaOH without inhibitor (Blank) and with 2.0 gm/dL AILE (AI).

### 3.1.9 Mechanism of corrosion inhibition by Azadirachta indica leaves extract:

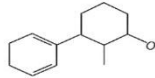
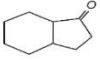
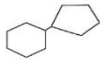
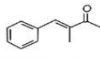
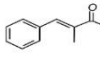
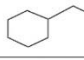
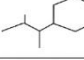
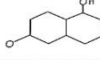
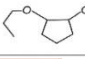
The extract acts as an efficient and eco-friendly corrosion inhibitor for aluminium metal in alkaline media such as NaOH solution. Numerous bioactive substances, such as flavonoids (quercetin, kaempferol), alkaloids (nimbin, nimbidin), terpenoids (azadirachtin, salannin), tannins, saponins, and steroids ( $\beta$ -sitosterol), are detected in neem leaves using phytochemical screening[48] Through donor-acceptor interactions and electrostatic attraction, these compounds' numerous  $\pi$ -electron systems and heteroatoms like nitrogen and oxygen enable them to adsorb strongly onto the aluminium surface[49]. By creating an adsorbed protective layer made of organic molecules, Azadirachta indica leaf extract dramatically lowers the pace at which aluminium corrodes in NaOH media. This layer minimizes metal breakdown by preventing hydroxide ions and dissolved oxygen from diffusing to the aluminium surface. Because phytochemicals cover more surface, the inhibitory efficacy rises with extract concentration [50]. Adsorption stability is improved by the presence of substances like quercetin, nimbin, and azadirachtin through chelation and synergistic interaction with the aluminium oxide layer [51].

The inhibition efficiency increases with extract concentration due to more phytochemicals adsorbing on the metal surface. Together, these substances create a dense organic layer that obstructs active corrosion sites, protecting the surface. Metal-inhibitor bonding is promoted by the presence of several functional groups ( $-\text{OH}$ ,  $-\text{OCH}_3$ ,  $\text{C}=\text{O}$ ), which increase electron donation [49].

These phytochemicals are adsorbed on the aluminium surface when AILE is added to NaOH solution. This results in the formation of a compact and adherent organic coating that

serves as a chemical and physical barrier between the metal and the corrosive environment. This barrier delays the oxidation of aluminium to aluminate species and stops hydroxide ions ( $\text{OH}^-$ ) from attacking [50]. The inhibition efficiency rises with extract concentration, suggesting that the inhibitor molecules enhanced surface covering is what controls corrosion.

The Langmuir adsorption isotherm is typically followed by the adsorption of AILE components, indicating monolayer adsorption on the metal surface. Additionally, azadirachtin, quercetin, and nimbin work in concert to improve film stability and inhibitory performance [51].

Compound	Molecular Formula	Class	Structure / Activity
Azadirachtin	$\text{C}_{35}\text{H}_{44}\text{O}_{16}$	Terpenoid (limonoid)	
Nimbin	$\text{C}_{30}\text{H}_{30}\text{O}_9$	Alkaloid (limonoid-type)	
Nimbidin	$\text{C}_{27}\text{H}_{30}\text{O}_9$	Alkaloid	
Quercetin	$\text{C}_{15}\text{H}_{10}\text{O}_7$	Flavonoid	
Kaempferol	$\text{C}_{15}\text{H}_{10}\text{O}_6$	Flavonoid	
Salannin	$\text{C}_{34}\text{H}_{44}\text{O}_9$	Terpenoid (limonoid)	
$\beta$ -Sitosterol	$\text{C}_{29}\text{H}_{50}\text{O}$	Steroid	
Tannins (generic)	Polyphenolic	Polyphenolic	
Saponins (generic)	Glycoside-type	Glycoside	

**Fig. 11:** Structure of main phytoconstituents of AILE.

Overall, the extract from AILE reduces both anodic dissolution and cathodic hydrogen evolution, acting as a mixed-type inhibitor. AILE is a sustainable and eco-friendly green inhibitor for aluminium in NaOH medium because it forms a hydrophobic protective layer that dramatically lowers the rate of corrosion.

#### 4. Conclusion:

The results of this study demonstrate that increasing the concentration of inhibitors leads to a decrease in the corrosion rate and a corresponding increase in inhibition efficiency at a constant base concentration. Conversely, increasing the base concentration results in a higher corrosion rate and reduced inhibition efficiency at a fixed inhibitor concentration. The adsorption of inhibitor molecules on the aluminium surface follows the Langmuir adsorption isotherm, as confirmed by the linear relationship between 'C' vs 'C/ $\theta$ ' with an approximately

unit slope, indicating monolayer adsorption. The higher activation energy ( $E_a$ ) values observed for inhibited systems compared to uninhibited ones suggest that the inhibitors are more effective at lower temperatures. The negative values of Gibbs free energy of adsorption ( $\Delta G_{ads}$ ) and heat of adsorption ( $\Delta Q_{ads}$ ) indicate that the adsorption process is spontaneous and exothermic. However, the positive values of enthalpy change ( $\Delta H_a$ ) imply that the corrosion process is favoured at higher temperatures, while the positive entropy change ( $\Delta S_a$ ) indicates that the process is entropically favourable. Surface analysis using SEM reveals that the aluminium surface in the presence of inhibitors is smoother than that of the uninhibited system, confirming the formation of a protective film. EDX analysis further supports this by showing characteristic peaks corresponding to green inhibitor compounds. Moreover, the inhibition efficiency values obtained from mass loss, electrochemical polarization, and electrochemical impedance spectroscopy (EIS) methods are in good agreement. Overall, the findings confirm that *Azadirachta indica* leaf extract is an effective corrosion inhibitor for aluminium in NaOH solution.

#### **Acknowledgement:**

The authors are thankful to the Department of Chemistry, C. B. Patel Computer College & J.N.M. Patel Science College, Surat, for providing laboratory facilities. Authors are also thankful to **The National Fellowship & Scholarship for Higher Studies of ST students (Being implemented by the Ministry of Tribal Affairs, Government of India) for financial assistance.**

#### **Reference:**

- Zhang J., Klasky M. and Letellier B. C., *J. of Nuclear Materials*, 175-189, (2009).
- Pyun S. and Moon S., *J. of Solid State Electrochemistry*, 4, 267–272, (2000).
- Amin M. A., El-Rehim SS Abd, El-Sherbini E. E. F., Hazzazi O. A. and Abbas M. N., *Corrosion Science*, 51, 658-667, (2009).
- Doche M. L., Novel-Cattin F., Durand R. and Rameau J. J., *J. of Power Sources*, 65, 197-205, (1997).
- Abdel-Gaber M., Khamis E., Abo-Eldahab H. and Adeel S., *Materials Chemistry and Physics*, 124, 773-779, (2010).
- Hussein H., Sahlanee Al and Sultan Abdul-Wahab A., *Aquatic Science and Technology*, 1(2), 135-150, (2013).
- Arockiasamy P., Queen Rosary Sheela X., Thenmozhi G., Franco M., Wilson S. J. and Jayasanthi R., *Int. J. of Corrosion*, 7, (2014).

- Rodriguez-Clemente E., Gonzalez-Rodriguez J. G. and Valladares-Cisneros M. G., *Int. J. Electrochem. Sci.*, 9, 5924-5936, (2014).
- James A. O. and Akaranta O., *Res. J. Chem. Sci.*, 1(1), 31-37, (2011).
- Agu P. C. and Okon K., *Zastita Materijala*, 64(3), (2023).
- Prashanth G. K. and Krishnaiah G. M., *Int. J. Adv. Eng. Technol. Mgt Appl. Sci.*, 1(5), 21-31, (2014).
- Abakedi O. U. and Asuquo J. E., *J. Basic and Applied Research*, 2(4), 556-560, (2016).
- Selvam N. V., Sharma A. and Ramachandran M., *Period. Polytech. Chem. Eng.*, 67(3), 396-406, (2023).
- Ameh E. M., Ekwoba L., Ocheme G. W., Oteno F., Umar A. Y., Esseoghene E. L., *J. Mater. Environ. Sci.*, 16(2), 341-353, (2025).
- Loto R. T. and Akpanyung K., *E3S Web of Conf.*, 603, 02013, (2025).
- Malarvizhi M., Sivakumar D. and Jaganathan M., *Asian J. Chem.*, 30(9), 1953-1960, (2018).
- Patel B. B. and Vashi R. T., *J. Appl. Chem.*, 6(3), 340-349, (2017).
- Patel K. K. and Vashi R. T., *Res. J. Chem. Sci.*, 5(11), 59-66, (2015).
- Ade S. B., *Int. J. Res. Appl. Sci. & Eng. Tech. (IJRASET)*, 10(III), 136-147, (2022).
- Lakshmi P. K., Rajam S. and Subramania A., *J. Chem. Pharm. Res.*, 4, 337, (2012).
- El Etre A. Y., Abdallah M. and El-Tantawy Z. E., *Corros. Sci.*, 47(2), 385-395, (2005).
- Deyas M. A., *J. Ind. and Eng. Chem.*, 22, 384-389, (2015).
- Halambek J., Zutinic A. and Berkovic K., *Int. J. Electrochem. Sci.*, 8, 11201-11214, (2013).
- Bruker G. R. and Phipps P. B., *Corrosion Chemistry ACS.*, 293, (1979).
- Lebrini M., Robert F. and Ross C., *Int. J. Electrochem. Sci.*, 5(11), 1698, (2010).
- Thomson R. H., "Naturally Occurring Quinones", 3<sup>rd</sup> ed., Academic Press, London, New York, 74, (1971).
- Martinez J. S. and Matikos-Hukovic M., *J. Appl. Electrochem.*, 33, 1137-1147, (2003).
- Subramanian N. and Ramkrishna K., *Indian J. of Technology*, 8, 369, (1970).
- Khaled K. F., *Electrochim. Acta.*, 48, 2493, (2003).
- Mu G., Li X. and Liu G., *Corros. Sci.*, 47, 1932, (2005).
- Oguzie E. E., *Corros. Sci.*, 50(11), 2993, (2008).
- Popova A., Sokolova E., Raicheva S. and Christov M., *Corros. Sci.*, 45(1), 33, (2003).

- Desai S. A. and Patel K. K., *IJRAR*, 12(3), 489-498, (2025).
- Desai S. A. and Patel K. K., *JETIR*, 13(1), a741-a748, (2026).
- Ibrahim T., Alayan H. and Al Mowaqet Y., *Prog. Org. Coat*, 75, 456, (2012).
- Ansari K. R., Yadav D. K., Ebenso E. E. and Quraishi M. A., *Int. J. Electrochem. Sci.*, 7(5), 4780-4799, (2012).
- Yaro A. S., Khadom A. A. and Ibraheem H. E., *Anti Corrosion Methods and Materials*, 58(3), 116-124, (2011).
- Prasanna B. M., Praveen B. M., Hebbar N. and Venktesha T. V., *J. Fund. Appl. Sci.*, 7(22), 222-243, (2015).
- Issa R. M., El-Sonbati A. Z., El-Bindary A. A. and Kera H. M, *Eur. Polym. J.*, 38(3), 561-566, (2002).
- Talati J. D. and Modi R. M., *Trans. SAEST*, 11, 259, (1986).
- Ebenso E. E., *Bull. Electrochem.*, 20, 551, (2004).
- Rout P. K. and Sahu S. N., *Surface Eng. and Applied Electrochem.*, 53(2), 190-197, (2017).
- Singh A. K. and Ebenso E. E., *Materials J. of and Env. Science*, 2(4), 415-425, (2011).
- Quraishi D. and Singh R., *J. of Ind. Che.*, 45, 125-133, (2018).
- Quraishi M. A., Ansari F. A. and Jamal D., *Mater. Chem. Phy.*, 77, 687-690, (2003).
- Li W., Zhao X., Liu F. and Hou B., *Corros. Sci.*, 50, 3261-3266, (2008).
- Desai P. S., Parmar B, Desai F. P. and Patel A., *Results in Surfaces and Interfaces*, 14, (2023).
- Prakash D. and Gupta C., *Natural Product Research*, 28(17), 1450-1465, (2014).
- Sastri V. S., “Green Corrosion Inhibitors: Theory and Practice”, Hoboken, NJ: John Wiley & Sons, (2011).
- Bharathi S., Jeyaprabha, C. and Prakash P., *Materials Today: Proceedings*, 18, 1736-1743, (2019).
- Abiola O. K. and Tobun Y., *Chemical Engineering Communications*, 197, 1029-1042, (2010).